

Recent progress in optoelectronic neuromorphic devices

Yan-Bo Guo(郭延博), Li-Qiang Zhu(竺立强)

Citation: Chin. Phys. B . 2020, 29(7): 078502 . **doi:** 10.1088/1674-1056/ab99b6
Journal homepage: http://cpb.iphy.ac.cn; http://iopscience.iop.org/cpb

What follows is a list of articles you may be interested in

Thickness-modulated in-plane Bi_2O_2Se homojunctions for ultrafast high-performance photodetectors

Cheng-Yun Hong(洪成允), Gang-Feng Huang(黄刚锋), Wen-Wen Yao(要文文), Jia-Jun Deng(邓加军), Xiao-Long Liu(刘小龙)

Chin. Phys. B . 2019, 28(12): 128502 . **doi:** 10.1088/1674-1056/ab4e87

Transition of photoconductive and photovoltaic operation modes in amorphous Ga_2O_3-based solar-blind detectors tuned by oxygen vacancies

Yan-Fang Zhang(张彦芳), Xuan-Hu Chen(陈选虎), Yang Xu(徐阳), Fang-Fang Ren(任芳芳), Shu-Lin Gu(顾书林), Rong Zhang(张荣), You-Dou Zheng(郑有炓), Jian-Dong Ye(叶建东)

Chin. Phys. B . 2019, 28(2): 028501 . **doi:** 10.1088/1674-1056/28/2/028501

Metal halide perovskite photodetectors: Material featuresand device engineering

Ye Wang(王烨), Meng-Lei Gao(高孟磊), Jin-Liang Wu(吴金良), Xing-Wang Zhang(张兴旺)

Chin. Phys. B . 2019, 28(1): 018502 . **doi:** 10.1088/1674-1056/28/1/018502

Time-dependent crosstalk effects for image sensors with different isolation structures

Lei Shen(沈磊), Li-Qiao Liu(刘力桥), Hao Hao(郝好), Gang Du(杜刚), Xiao-Yan Liu(刘晓彦)

Chin. Phys. B . 2018, 27(8): 088503 . **doi:** 10.1088/1674-1056/27/8/088503

Organic photovoltaic cells with copper (Ⅱ) tetra-methyl substituted phthalocyanine

Xu Zong-Xiang, Roy V. A. L.

Chin. Phys. B . 2013, 22(12): 128505 . **doi:** 10.1088/1674-1056/22/12/128505

TOPICAL REVIEW — Physics in neuromorphic devices

Recent progress in optoelectronic neuromorphic devices*

Yan-Bo Guo(郭延博)[1,2,3] and Li-Qiang Zhu(竺立强)[1,2,†]

[1] School of Physical Science and Technology, Ningbo University, Ningbo 315211, China
[2] Ningbo Institute of Materials Technology and Engineering, Chinese Academy of Sciences, Ningbo 315201, China
[3] School of Materials Science & Engineering, Shanghai University, Shanghai 200444, China

(Received 2 April 2020; revised manuscript received 21 May 2020; accepted manuscript online 5 June 2020)

Rapid developments in artificial intelligence trigger demands for perception and learning of external environments through visual perception systems. Neuromorphic devices and integrated system with photosensing and response functions can be constructed to mimic complex biological visual sensing behaviors. Here, recent progresses on optoelectronic neuromorphic memristors and optoelectronic neuromorphic transistors are briefly reviewed. A variety of visual synaptic functions stimulated on optoelectronic neuromorphic devices are discussed, including light-triggered short-term plasticities, long-term plasticities, and neural facilitation. These optoelectronic neuromorphic devices can also mimic human visual perception, information processing, and cognition. The optoelectronic neuromorphic devices that simulate biological visual perception functions will have potential application prospects in areas such as bionic neurological optoelectronic systems and intelligent robots.

Keywords: artificial synapses, optoelectronic devices, neuromorphic devices, visual perception systems

PACS: 85.60.−q, 85.60.Dw **DOI:** 10.1088/1674-1056/ab99b6

1. Introduction

With the rapid development of artificial intelligence (AI) and Internet of things (IoTs), special requirements are arisen for computation speed and energy consumption.[1,2] Unfortunately, it is hard to satisfy the increasing demands of computation resources with the coming of information explosion by the traditional computation systems based on von Neumann architectures, where the physical separation of memory module and processing module brings about limited data transmission rate and huge energy consumption.[3,4] As comparison, our brain consists of $\sim 10^{11}$ neurons and $\sim 10^{15}$ synapses. Neurons and synapses are the basic units of brain memory and information processing.[5] They can execute computation in a parallel model. Thus, unstructured tasks such as perception, learning, thinking, memory, and decision-making can be fulfilled in an energy efficient pattern due to the highly parallel, event-driven, and energy-efficient architectures.[6,7] Therefore, brain inspired computation configurations are proposed to overcome the von Neumann bottleneck. Moreover, neuromorhpic devices are considered as a feasible technical way to realize the brain-like computation in artificial neural networks (ANNs) and artificial intelligence.[8] In the last decade, two-terminal resistance switching devices (e.g., memristors,[9–12] phase change memories[13]) and three-terminal transistors (e.g., ferroelectric transistor,[14] electrolyte gated transistors,[15–22] memtransistors[23]) have been proposed for neuromorhpic device applications. Several biological synaptic plasticity behaviors have been mimicked, including paired pulse facilitates (PPF), synaptic filtering, spike-timing dependent plasticity (STDP), metaplasticity, etc. Moreover, neural calculations have been simulated successfully, including pattern memory,[24,25] pattern recognition,[26,27] reservoir computing,[28] spatiotemporal dynamic logic,[15,16,29–31] etc.

A peripheral nervous system can sense and respond to external stimuli such as light, sound, pressure, and chemicals. This sensation information can be transferred to the central nervous system.[32] Previously, pressure sensors[33] and electronic skin (E-skin) devices[34] have successfully simulated the touch response of human skin. Recently, tactile sensing characteristics have been achieved by connecting pressure sensor with neuromorphic transistor or neuromorphic memristor, possessing the functions of signal conversion and information processing.[10,11] Such bionic tactile sensing systems based on neuromorphic devices will have broad application prospects in low-cost bionic smart field information sensing and intelligent identification. We receive most of outer information through our visual perception systems.[35] The photoreceptors in the retina receive light inputs and convert them into electrical signals. The optic nerves, composed of various neu-

*Project supported by the National Natural Science Foundation of China (Grant No. 51972316), Open Project of State Key Laboratory of ASIC & System (Grant No. 2019KF006), Zhejiang Provincial Natural Science Foundation of China (Grant No. LR18F040002), and Program for Ningbo Municipal Science and Technology Innovative Research Team, China (Grant No. 2016B10005).

†Corresponding author. E-mail: zhuliqiang@nbu.edu.cn

© 2020 Chinese Physical Society and IOP Publishing Ltd

rons and adjacent synapses, can transmit the electrical stimuli to the visual cortex. Recently, designing artificial visual perception system is attracting increasing interests. The main functions of the visual perception system include perception, learning, and memory of external information. Kwon *et al.*[36] designed a light-adjusted optoelectronic neuromorphic circuit consisted of a photovoltaic divider and an ionotronic synaptic transistor. The photovoltaic divider and synaptic transistor act as artificial retina and optic nerve, respectively. The light-adaptable synaptic functions of the biological visual perception system have been simulated successfully. In addition, photodetectors can also simulate artificial photoreceptors to obtain visual information by converting light signals into electrical signals.[37,38] At the same time, photoelectric neuromorphic devices with photosensitivity can directly convert light stimuli into post-synaptic signals to simulate visual perception learning systems. Recently, optoelectronic neuromorphic devices based on two-terminal memristors or three-terminal transistors have been demonstrated using different materials, such as metal oxides,[39,40] carbon nanotubes,[41] graphene,[42] and MoS_2.[43] Compared with electrical signals, optical signals can be regarded as additional terminals, which greatly enrich the degree of freedom in regulating the synaptic plasticity. Therefore, bionic systems that combine optoelectronic neuromorphic devices, bionic prostheses, and soft robotics will greatly advance the development of artificial intelligence systems.

Here, we describe the optoelectronic characteristics of two-terminal memristors and three-terminal transistors. Photo-illumination triggered synaptic responses and neural cognitive behaviors are discussed. Later, integration of artificial visual perception and artificial biological systems is described, reflecting the trend of future bionic neural networks. Finally, a short outlook is provided. Table 1 shows synaptic functions achieved on optoelectronic neuromorphic devices.

Table 1. Synaptic functions achieved on optoelectronic neuromorphic devices.

Light-induced synaptic functions	Optoelectronic neuromorphic memristors	Optoelectronic neuromorphic transistors
Excitatory post-synaptic current (EPSC)	[44–47]	[48,49]
Paired pulse facilitates (PPF)	[44,45,47,50]	[51,52]
Inhibitory post-synaptic current (IPSC)	[45]	[53–55]
Long-term plasticity	[39,45,47,56]	[51,52,57]
Spike-timing dependent plasticity (STDP)	[58]	[52–55,59,60]
Visual memory	[40,43,46,61]	[36,51]
Image recognition	[46]	[14,47,55,62]
Logic functions	[63,64]	[53,55,65]
Classical conditioning experiment	–	[54,59,65]

2. Optoelectronic neuromorphic memristors

The concept of memristor was first proposed by Professor Chua from the University of California, Berkeley in 1971.[66] In 2008, HP laboratories successfully manufactured TiO_2 based memristor.[67] Memristor is a two-terminal device with a three-layer structure, including top electrode (TE), bottom electrode (BE), and resistive switching (RS) layer. The resistance state can be changed by the amount of charges flowing through the RS layer. Memristors have advantages including simple physical structure, small size, non-volatile properties, memory capacity, low energy consumption, and good scalability. Up to date, various types of memristors have been reported, such as phase change memories (PCMs),[68] resistive switch memories,[69,70] etc. Due to the non-linear electrical properties, memristors have been proposed for artificial synapse and neuromorphic engineering applications.

2.1. Synaptic plasticities

As an interesting optoelectronic technology, photonic memories have attracted increasing attention in the last few years. Such devices have great potentials to overcome the von Neumann bottleneck. Moreover, integrated systems consisted of arrayed photonic memories have attracted increasing interests for adoption as building blocks in the biospired vision system.[71]

ZnO is a typical wide band gap semiconductor material with a band gap of ~ 3.37 eV. It has high exciton binding energy and excellent selective absorption of ultraviolet (UV) light. Thus, it has broad application prospects in ultraviolet detectors due to the significant photoelectric performances. As typical functional materials in microelectronic field, ZnO has also been proposed as RS layer in memristor. Recently, ZnO nanorods have been proposed for optically modulated artificial synapse applications.[44] The high resistance state (HRS) of the device is non-volatile, while the low resistance state (LRS) is volatile. This volatile characteristic is beneficial for simulating the short-term synaptic plasticity behavior. The HRS and LRS overlap immediately when exposing to UV illumination, as shown in the yellow part in Fig. 1(a). Since the decay kinetics in the light-excited LRS is similar to that in the electric-excited LRS, it is hardly to tell whether the device was in LRS or HRS before illumination. Such light-induced shielding of

HRS and LRS is called optical shielding (OS). When a series of electric pulses are applied, the overlapped LRS and HRS show different responses and become discernible again, as shown in the blue part of Fig. 1(a). This process is called electrical shielding (ED). Such OS and ED functions can be used to encrypt and decrypt data, respectively, making it possible to process massive data for ANN applications. In such a device, oxygen vacancies are distributed along the surfaces of the vertically aligned nanorods, which helps the unique electrical characteristics.

Furthermore, ZnO_{1-x}/AlO_y heterojunction based photoelectric memristor has also been proposed with ITO/ZnO_{1-x} /AlO_y/Al stacks.[39] Here, the AlO_y layer is naturally formed on Al. The device shows typical current–voltage (I–V) sweeping curves in the dark and under UV-light illumination, displaying LRS and HRS. The operation mechanism is related to the electron trapping/detrapping at the trapping sites in the AlO_y layer. Under negative bias, an electron depletion layer is formed in the AlO_y layer, realizing a reset process from the LRS to the HRS. Under positive bias, the depletion layer will get narrow, which causes LRS. While the UV-light illumination modulates the resistive behaviors due to photogenerated holes and persistent photoconductivity effects. Thus, the device can demonstrate photoelectric plasticity by setting light pulse stimulation at different pulse width, pulse intensity, pulse number, and pulse frequency. Figure 1(b) shows the conversion from short-term plasticity to long-term plasticity by changing the optical power density of the light pulse. As a typical form of short-term plasticity, paired pulse facilitate (PPF) plays an important role in processing temporal auditory or visual information.[72] Figure 1(c) shows the PPF behavior simulated on the memristor under light stimuli. Moreover, neuromorphic facilitation, depression and long-term plasticity have been mimicked on the device.

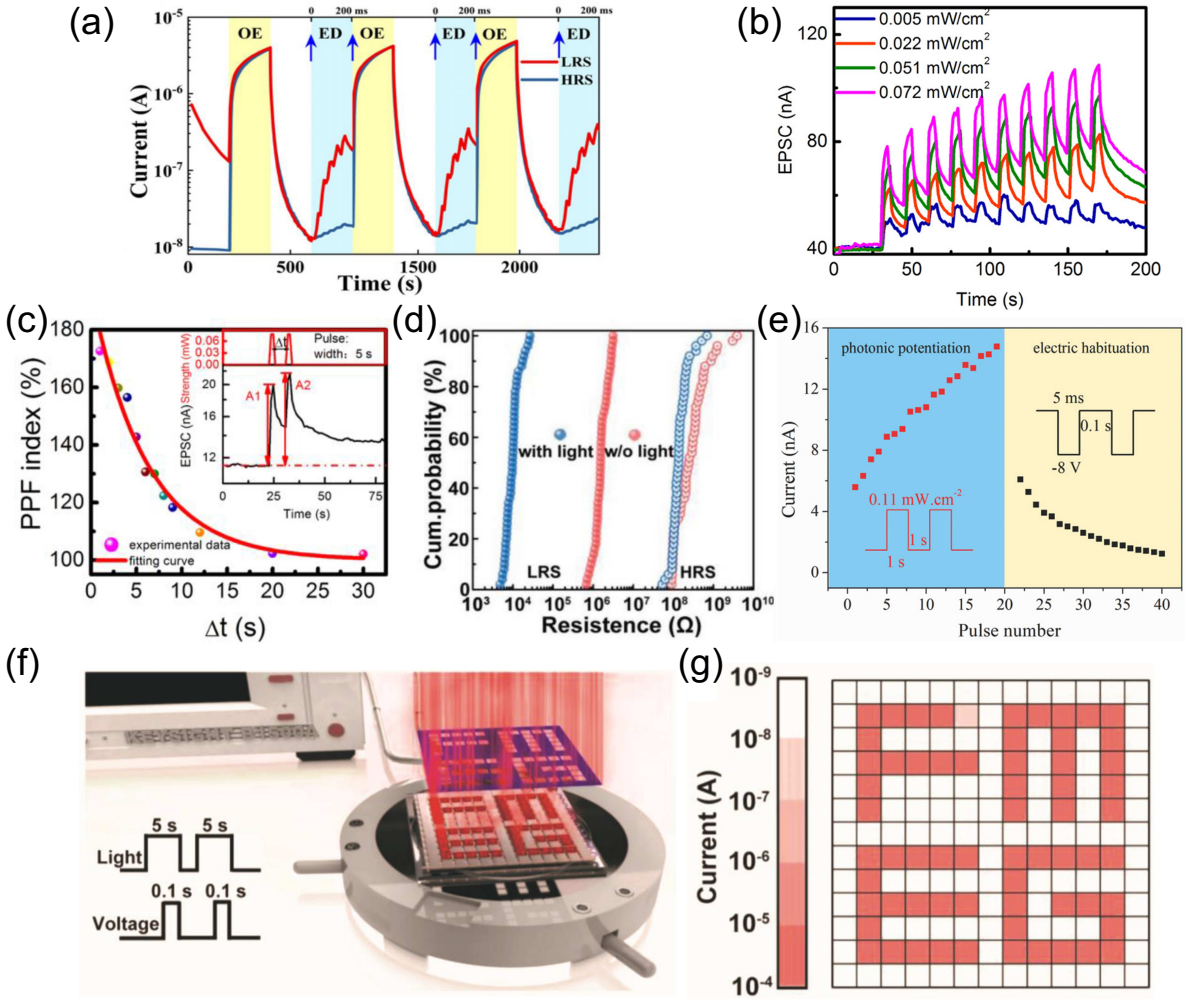


Fig. 1. Optoelectric neuromorphic memristors for neuromorphic applications. (a) Optical shielding (OS) and electrical deshielding (ED) of the memristor based on a vertically arranged ZnO nanorod structure. The blue arrows indicate the time scale of the ED process. (b) Photonic EPSC behavior under different light pulse power density. The read voltage is 0.1 V. (c) Photonic PPF behavior. (d) Cumulative probability plot of resistance measured for 150 times on 15 different samples under NIR and dark conditions. (e) Photonic potentiation and electric habituation in the W/MoS_2/p-Si memristive synapse. (f) System integration of the RRAM array with light signal. (g) The light signals are stored in the 13×13 RRAM array. (a) Reprinted with permission from Ref. [44], Copyright 2018, AIP Publishing. (b) and (c) Reprinted with permission from Ref. [39], Copyright 2018, American Chemical Society. (d), (f), and (g) Reprinted with permission from Ref. [43], Copyright 2018, Wiley-VCH. (e) Reprinted with permission from Ref. [45], Copyright 2018, Wiley-VCH.

Two-dimensional (2D) transition metal dichalcogenides (TMDs) are considered as promising candidates for the next generation optoelectronics and photodetection due to their unique electrical, mechanical, and optical properties.[45,73] Especially, they have also been proposed for photonic memristor applications with light illumination at near-infrared region (NIR) due to the small band gap, showing great potentials in memristive synapses. Due to the combination of photonic and electric neuromorphic functions, they would have prospectives in synthetic retinas and optoelectronic interfaces. Zhai *et al.*[43] used a heterostructure formed with upconversion nanoparticles (UCNPs) and molybdenum disulfide (MoS_2) to achieve optically tunable memory performance under NIR illumination. The upconversion material has excellent light response performances in the NIR due to its photon conversion characteristics.[74,75] With the increased light intensity, both the SET voltage and the RESET voltage gradually decrease. While the ON current and OFF current increase correspondingly. Figure 1(d) shows the cumulative probability plot of resistance measured for 150 times on 15 different samples under NIR and dark conditions. Such NIR light tunable behavior lays the foundation for the application of multifunctional memory devices. Furthermore, memory functions of photon write-electric erase can also be implemented based on photonic potentiation and electric habituation characteristics.[45] For W/MoS_2/p-Si memristive synapse, the increase of the conductance corresponding to EPSC can be used to mimic the potentiation of the synaptic strength, while the decrease of the conductance corresponding to IPSC can be used to mimic the habituation of the synaptic strength. A continuous optical pulse sequence (power intensity: 0.11 mW/cm^2, width: 1 s) gradually increases the conductances due to the photogenerated electrons and holes, as shown in Fig. 1(e). This behavior simulates the potentiation of the synaptic strength. While a continuous negative voltage pulse sequence (amplitude: −8 V, width: 5 ms) gradually decreases the conductances, thus mimicking the habituation of the synaptic strength. In addition, synaptic potentiation and habituation behaviors can be modulated by changing the amplitude or width of light and electrical pulse stimuli.

2.2. Visual memory

In human visual system, eyes can receive image information from retina. And the optic nerve can transfer visual signals to the visual center to form visual memory. Figure 2(a) schematically shows the whole process. Such visual perception system can be simulated by integrating memory devices and image sensors. Shen *et al.*[40] proposed a memristor system to imitate human visual memory by integrate UV resistive image sensors and resistive switching memory devices. Figure 2(b) schematically shows the bioinspired visual memory unit. The In_2O_3 micrometer-sized wires array is used to detect the UV signals. Ni/Al_2O_3/Au memristor is fabricated to connect the photosensor and to store the detected optical signals. The flexible visual memory arrays fabricated on PI substrate are composed of 10×10 pixels. When UV light is applied, the memristor will be programmed. When the light is removed, the memristor has been programmed to a non-volatile state. In another word, the stored information of light distribution on the pixel shows long-term retention performances due to

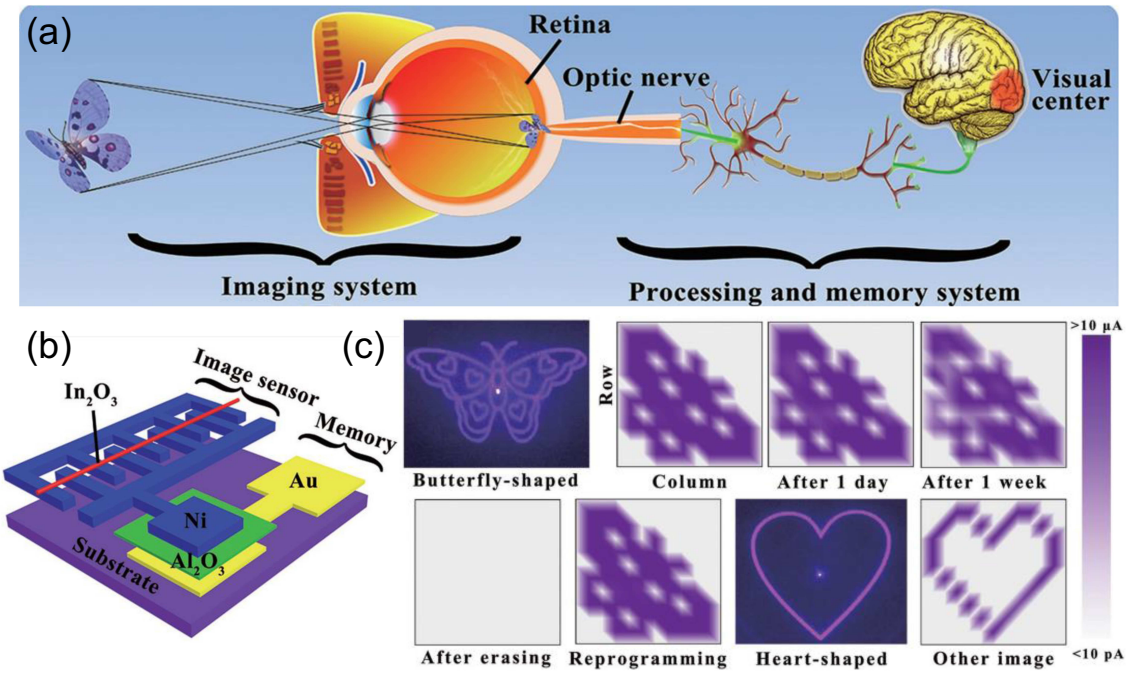


Fig. 2. Artificial visual memory. Schematic illustration of (a) human visual memory system and (b) artificial visual memory device. (c) Information storage and reprogrammable capability of the visual memory device arrays. (a)–(c) Reprinted with permission from Ref. [40], Copyright 2018, Wiley-VCH.

the nonvolatile characteristic of the resistance switching memristor. Especially, the light image can be maintained for at least one week. When a UV image with a special pattern, for example a butterfly, has been received by the visual memory arrays, the pattern will be memorized, as shown in Fig. 2(c). When applying negative voltage on the memrsistor, the visual memory arrays can be programmed again, i.e., the resistance state is switched from LRS to HRS. In another word, the stored light information can be erased. Thus, the visual memory arrays can be re-used for a new image. Visual memory function can also be mimicked directly on optoelectronic memory device arrays. As discussed in the previous part that the heterostructure of UCNPs/MoS_2 can achieve optically tunable memory performance under NIR illumination.[43] Thus, the sensor and the visual memory can be realized on the single optoelectronic memristor. Figure 1(f) schematically shows 13×13 optomemory arrays. Pattern characters "FMEG" can be written into the arrays under the assistance of NIR illumination. Whereafter, the resistance states of the memory arrays can be read out electrically at a read voltage of 0.5 V, as shown in Fig. 1(g). Moreover, Mennel *et al.*[76] proposed an ANN vision sensor for ultra-fast recognition and encoding of optical images. It provides various training possibilities for ultra-fast machine vision applications.

These optical-assistance storage systems can reapear the stored image information, and provide a novel approach to imitate human echoic memory and haptic memory. Moreover, the flexible visual memory device will have potentials in wearable electronics, electronic eyes, etc.

3. Optoelectric neuromorphic transistors

Transistors have also been proposed for neuromorphic device applications as early as in 1996 by Carver Mead[77] Due to unique characteristics of the three-terminal transistor, it has certain advantages over two-terminal device in terms of neuromorphic applications. Firstly, the information transfer and learning process can be executed synchronously. Second, the synaptic performance can be regulated by adding additional gates to amplify signals and reduce energy consumption. Thirdly, multi-gates can be integrated for realizing dendritic algorithm.[23,31,78,79] Therefore, three-terminal transistor based neuromorphic devices would act as fundamental building blocks in the field of synaptic bionics and neuromorphic computing. Especially, phototransistor would facilitate the co-regulation of semiconductor channel conductances by light and electrical stimuli. Thus, they would also have great potentials in artificial visual neuromorphic system.

3.1. Synaptic plasticities

The transmission of information between neurons depends on the delivery of neurotransmitters between synaptic clefts. The release of neurotransmitters leads to different kinds of synaptic functions, including synaptic potentiation and depression, excitatory post-synaptic current, paired pulse facilitation, synaptic filtering, short-term plasticity, long-term plasticity, etc. Thus, one of the main tasks for phototransistors in neuromorphic engineering applications would be the realization of these basic synaptic functions. In phototransistors, light stimuli are regarded as pre-synaptic spikes to trigger the synaptic responses. With smart designs and strategies, basic synaptic response and unique neural functions have been mimicked on these kinds of neuromorphic transistors.

Recently, layered 2D materials have been paid attention for neuromorphic system applications.[80,82,83] Kim *et al.*[80] designed MoS_2 phototransistors for optical synaptic device applications, as schematically shown in Fig. 3(a). P-type Ge acts as the back gate. When Ge absorbs light in the region from visible to infrared ($\lambda = 520$–1550 nm), band bending happens in Ge, which changes the modulation behaviors of the Ge back gate. It exhibited a fast rising time of 0.1 ms and a decay time of 45 ms for infrared light. The process could simulate the visual information identifications in retina. Both potentiation and depression behaviors have been demonstrated under different light illumination, including visible ($\lambda = 520$ nm), dark, and infrared ($\lambda = 1550$ nm), as shown in Fig. 3(b). The results indicate potentials in both optical-sensing and synaptic operations in one device. Recently, black phosphorus (BP) is also emerged as an exciting 2D material. The strong light–matter coupling brings great potentials in broadband photodetection (UV to infrared), demonstrating exotic electronic and optoelectronic properties. With distinctive photoresponse characteristics and strong light–matter coupling, BP has also been selected for applications in artificial synaptic devices, demonstrating both excitatory and inhibitory synaptic plasticity.[53,54] TAhmed *et al.*[54] reported an optically stimulated artificial synapse based on layered BP. The device can imitate both inhibitory and excitatory action potentials by applying optical stimulation. No additional alternating-polarity electrical stimuli are needed. Inhibitory post-synaptic current (IPSC) is also an important synaptic response in biological nerve system.[84] Thus, realization of inhibitory synaptic responses on hardware devices would be interesting for neuromorphic platforms.[85] The BP synaptic device demonstrates several kinds of neural functions, including spike-duration dependent plasticity (SDDP), short-term and long-term memory transitions, IPSC, EPSC, PPF, spatiotemporally correlated synaptic response, classical Pavlov's learning, and STDP. As shown in Figs. 3(c) and 3(d), both EPSC and IPSC behaviors have been demonstrated at different wavelengths of 280 nm and 365 nm, respectively. In the nerve system, it is observed that stimuli duration may affect the modulation of the synaptic response.[86]

The present device also demonstrates SDDP on both light induced EPSC and IPSC. Similarly, PPF behaviors have been mimicked by applying paired light stimuli. Ebbinghaus' forgetting curve, an important brain-like learning mechanism,[87] has also been mimicked on the device. By connecting two separate BP synaptic devices together, symmetric STDP responses have been mimicked by applying optical pulses on the two synaptic devices with certain pulse intervals. The energy consumption is estimated to be ~ 3.5 pJ per synaptic activity. Interestingly, the device would prone to unintentional optical exposures during multi-wavelength synaptic operations.

As discussed in the previous part, quantum dots (QDs) have been proved to be good choices in functional optoelectronic device applications. Photoresponse behaviors could be modulated by the sizes and the compositions of the QDs. The strategies have also great potentials in artificial light-sensitive synaptic devices. Recently, Huang *et al.*[81] reported a light-stimulated synaptic transistors (LSSTs) by blending inorganic halide perovskite quantum dots (IHP QDs) and organic semiconductors (OSCs) together. The device demonstrates improved charge separation efficiency of the photoexcited charges. Moreover, the IHP QDs/OSCs hybrid film demonstrates delayed decay in photocurrent, which is important for achieving synaptic performances. A light pulse (500 nm, 0.1 mW/cm^2, pulse width 500 ms) induces a typical EPSC response with peak EPSC value of ~ 1.3 nA, as shown in Fig. 3(e). When the pulse ends, the EPSC gradually decays back to rest state due to the slow recombination of the trapped electrons and holes. With the increased light pulse width, the

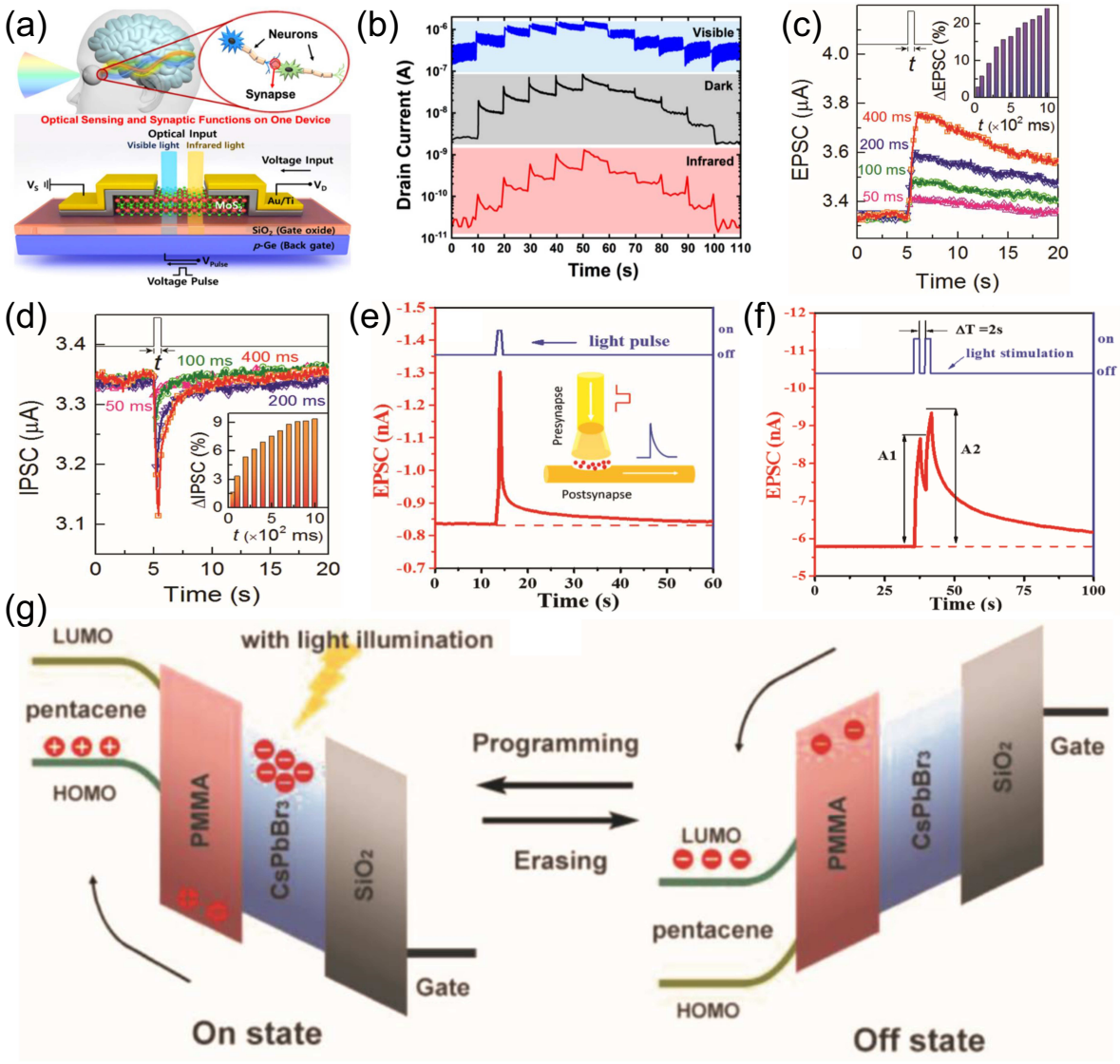


Fig. 3. Short-term plasticity on optoelectronic synapse transistors. (a) Schematic diagram of MoS_2 phototransistors based optical synaptic device. (b) Potentiation and depression behaviors obtained under different light conditions: visible ($\lambda = 520$ nm), dark, and infrared ($\lambda = 1550$ nm). (c) 280 nm optical stimulus-emulating EPSC. (d) 365 nm optical stimulus-emulating IPSC. (e) EPSC triggered by a light pulse. (f) EPSCs triggered by a pair of light pulses (500 nm, 0.1 mW/cm^2, $\Delta T = 2$ s). (g) Schematic diagram demonstrating light programming operation and electrical erasing operation for photonic flash memory based on all-inorganic $CsPbBr_3$ perovskite quantum dots (QDs). (a) and (b) Reprinted with permission from Ref. [80], Copyright 2019, American Chemical Society. (c)(f) Reprinted with permission from Refs. [54,81], Copyright 2019, Wiley-VCH. (g) Reprinted with permission from Ref. [37], Copyright 2018, Wiley-VCH.

EPSC increases correspondingly due to the increased photogenerated charges. When paired light pulses are introduced, the typical biological PPF function is also simulated on the LSSTs, as shown in Fig. 3(f). Photonic flash memory based on all-inorganic $CsPbBr_3$ perovskite QDs was also demonstrated.[37] The $CsPbBr_3$ QDs and semiconductor layer form a heterostructure to serve as a optically programmable and electrically erasable unit in the photonic flash memory. Figure 3(g) schematically shows the energy diagram under light programming operation and electrical erasing operation. During light illumination, large numbers of charge carriers are generated within the QDs layer. The photogenerated holes will escape to pentacene due to the energy band bending. Thus, photoinduced electrons will remain in the conduction band of the $CsPbBr_3$ QDs. Such trapped electrons can trigger an additional internal electric field to accelerate holes to be swept into the pentacene channel. When light illumination stops, such trapped electrons will be retained by the potential well with a long lifetime. Thus, such $CsPbBr_3$-based flash memory could be used to emulate information transmission in neuromorphic architectures. It is observed that the PPF index ratio decays with the increased optical pulse interval time. Moreover, it increases with the increased light intensity from 0.041 mW/cm^2, 0.069 mW/cm^2, 0.129 mW/cm^2 to 0.153 mW/cm^2. The observation is related to the fact that the increased light intensity promotes the generation of photoelectrons inside the $CsPbBr_3$ QDs and prolongs the decay time of the post-synaptic current (PSC). Furthermore, the device also demonstrates wavelength dependent synaptic plasticities.

It is interesting to note here that ionic-liquid or ionic-gel based electrolyte gated transistors (EGTs) can operate at low-voltage due to the unique interfacial ionic gating effects.[17,88–90] Interestingly, ion gating behaviors in EGTs are quite similar to those in biological synapse, which means that unique ion modulation behavior in EGTs could establish bridges between iontronic devices and neuromorphic platforms. Thus, there are several reports on ion-gated EGTs for neuromorphic device applications.[18–20,91] For example, starch-based bio-polysaccharide electrolyte gated indium–gallium–zinc oxide (IGZO) photoelectric synergic coupled neuromorphic transistors have been reported, demonstrating potentials in visual perception–learning system applications.[92] Figure 4(a) shows the schematic diagram of the device. The IGZO neuromorphic transistor demonstrates photon response activities. The photosensitivity (S) reaches a maximum value of $\sim 1.6 \times 10^7\%$ with V_{gs} at -0.45 V. When receiving light stimulus, the device demonstrates photo-electrical synergic synaptic responses. Figure 4(b) illustrates a typical PSC with absolute PSC amplitude of ~ 63 nA. When paired light pulses are applied, PPF behaviors are also demonstrated, as shown in Fig. 4(c). Interestingly, in the nervous system, synaptic response can be trigged by multiple pre-synaptic stimuli.[93] When different types of stimuli arrive in a temporal and spatial manner, a spatiotemporal integration phenomenon will happen in the neuron. The photoelectric synergic coupled neuromorphic transistors can also mimic synergic stimuli responses by applying photo-stimuli and electric stimuli in a temporal and spatial manner, as shown in Figs. 4(d) and 4(e). Thus, such photo-electrical synergic neuromorphic transistor will have potentials in bionic visual intelligent perception–learning system.

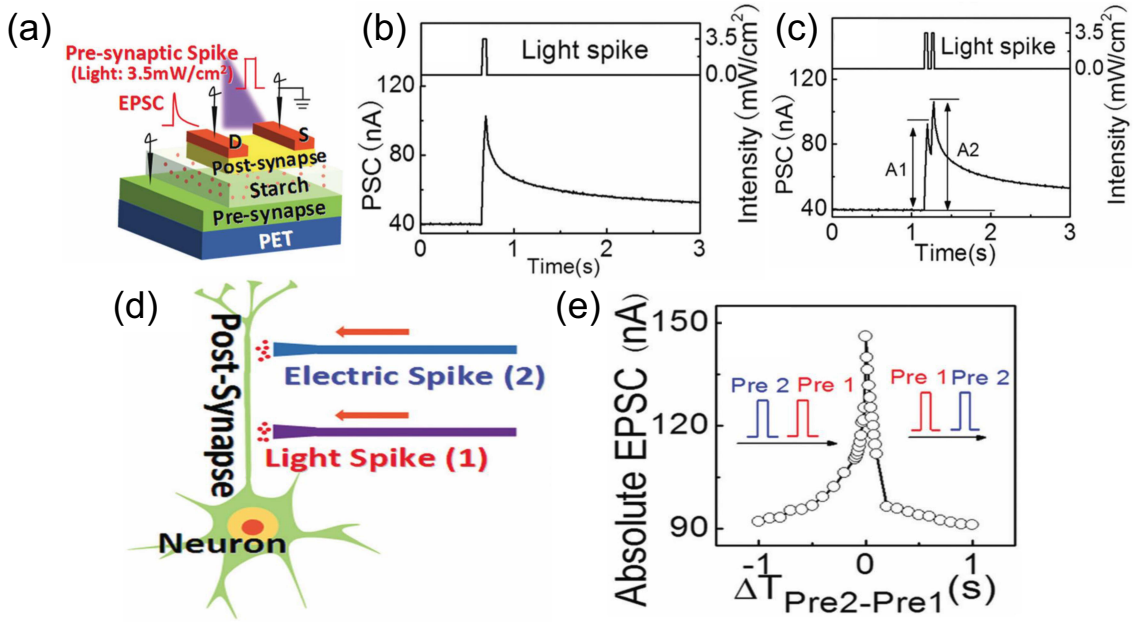


Fig. 4. Starch gated IGZO photoelectric neuromorphic transistors. (a) Schematic diagram of the device. (b) A typical post-synaptic current. (c) Typical PSC triggered with paired light pulses. (d) Schematic diagram of synergic effect in neurons activated by electric and light stimuli. (e) Absolute EPSC amplitude at zero time ($t = 0$) as a function of $\Delta T_{\text{Pre2}-\text{Pre1}}$. Reprinted with permission from Ref. [92], Copyright 2020, Royal Society of Chemistry.

3.2. Cognitive behaviors

In nervous system, synaptic plasticity is closely related to human brain learning and memory functions. In 1968, Atkinson and Shiffrin proposed a multistore model to explain the memory behavior.[94] The model describes three kinds of memories, including sensory memory (SM), short-term memory (STM), and long-term memory (LTM), as schematically shown in Fig.5(a). With frequent maintenance rehearsals, the memory level will be enhanced. In another word, SM can be transferred to STM and STM can be transferred to LTM with rehearsals. The phenomena of synaptic plasticity and transformation from STM to LTM have been mimicked on pn-junction-decorated IGZO phototransistors.[48] Figure 5(b) shows a transition from STP to LTP with the increased input light pulse intensity. The behavior is quite similar to the transition between STM and LTM with the increased electric spike amplitude observed on solid-state electrolyte gated oxide synaptic transistor.[95] Furthermore, a fading memory behavior is observed from the volatile part and nonvolatile part as shown in Fig. 5(c). STM-to-LTM transition has also been demonstrated on ITO/Nb:$SrTiO_3$ heterojunction artificial optoelectronic synapse by increasing the spike numbers or frequencies.[69] The current decay time and the steady current after decay also increase with the intensity, number, and frequency of the light pulse. In addition, both light pulse width and light pulse wavelength can also affect the transition characteristics between STM and LTM.[37,81]

Besides, there are two kinds of long-term synaptic plasticity includes long-term potentiation (LTP) and long-term depression (LTD).[96] The short-term synaptic plasticity provides temporary selection for neuron circuits, while LTP/LTD in synapses is the biological basis for continuous learning and memory. Thus, it is essential to mimic LTP and LTD to achieve cognitive complexity in artificial synapses. Qian *et al.*[97] achieved optical LTP and electrical LTD characteristics in optoelectronic synaptic device fabricated on a heterojunction consisted of copper-phthalocyanine (CuPc) and para-sexiphenyl (p-6P) layers. Figure 5(f) shows that the PSC increases linearly in the LTP area after applying 85 light pulses (width of 0.5 s and wavelength of 365 nm). Subsequently, the PSC in the LTD region drops non-linearly to the initial value after applying 85 electrical pulses (magnitude of −10 V, width of 0.1 s). The LTD behavior selectively leads to the decline of learning and memory. The LTP/LTD characteristic curves depend greatly on the light pulse conditions. The transition between LTP and LTD could be also realized by obeying spike-timing dependent plasticity (STDP) learning rules.

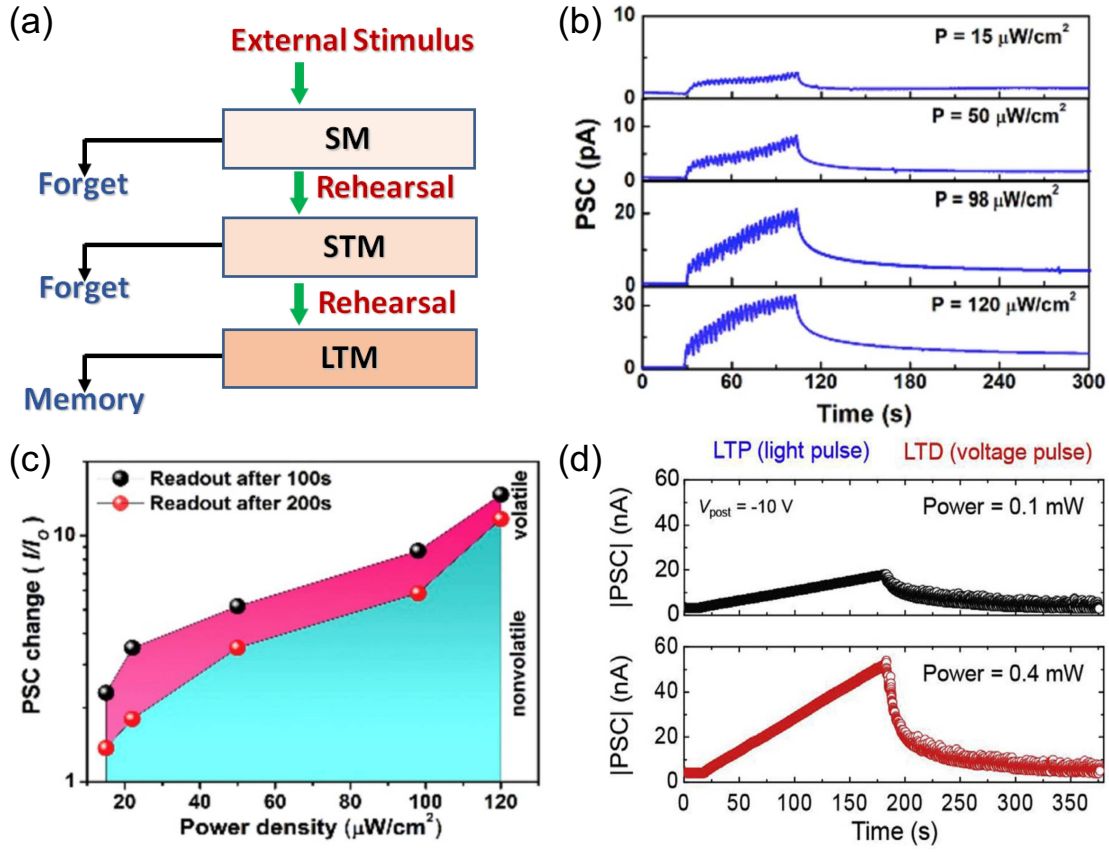


Fig. 5. Short-term memory (STM) and long-term memory (LTM). (a) Schematical diagram for the multistore model. (b) Continuous increase in PSC changes with the increased pulse intensity. (c) A fading memory behavior. (d) LTP/LTD characteristics of the CuPc/p-6P optoelectronic synapse for neuromorphic computing. (b) and (d) Reprinted with permission from Refs. [48,97], Copyright 2019, Elsevier.

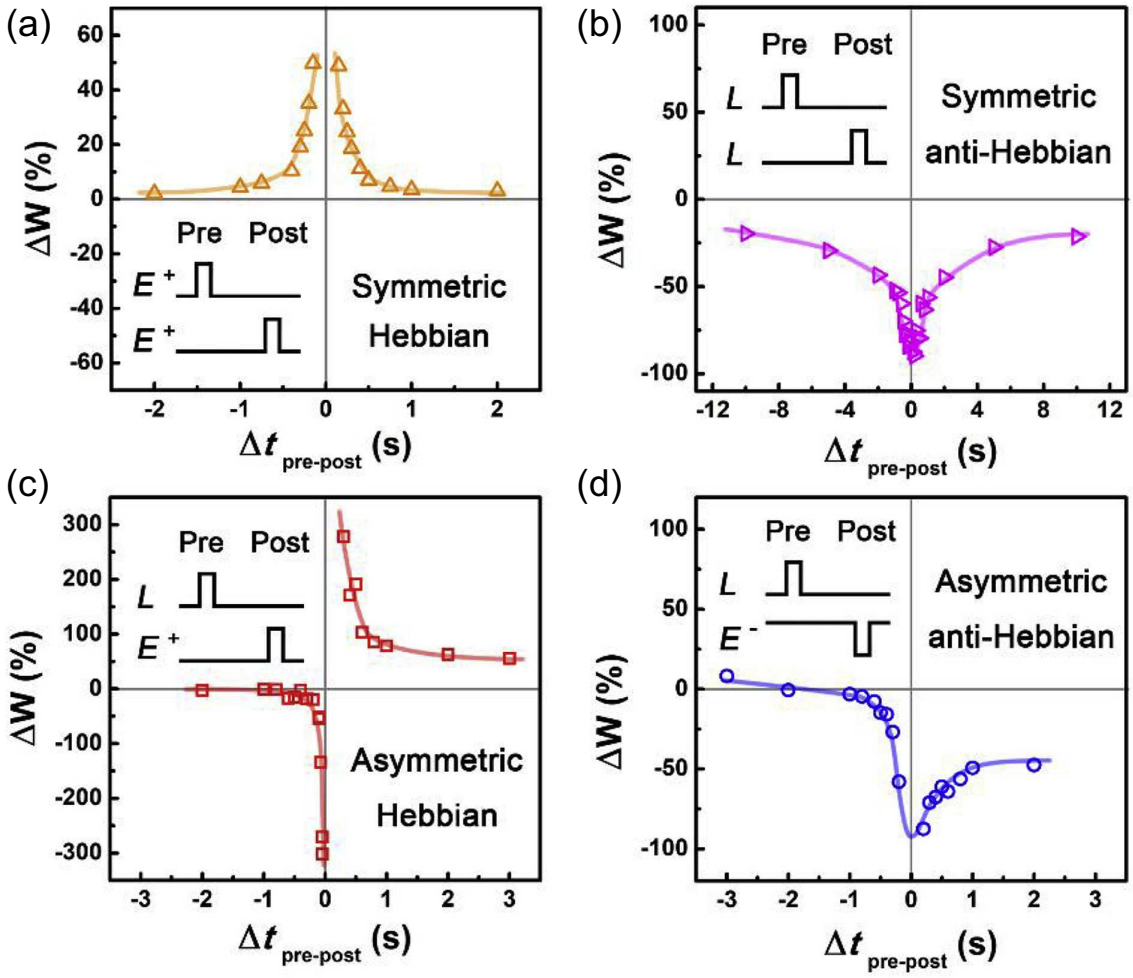


Fig. 6. Four kinds of STDP learning behaviors. (a) Symmetric Hebbian STDP rule. (b) Symmetric anti-Hebbian STDP rule. (c) Asymmetric Hebbian STDP rule. (d) Asymmetric anti-Hebbian STDP rule. Reprinted with permission from Ref. [55], Copyright 2019 Elsevier.

STDP plays a critical role in cognitive activities and determines the sign and magnitude of LTP or LTD. It refers to the change in synaptic weight with the interval time ($\Delta t_{\text{pre-post}}$) between pre-synaptic and post-synaptic spikes and is considered to be a key feature of synaptic plasticity in biological nervous system.[98,99] STDP is a complement to Hebbian synaptic plasticity and is considered to be the basis for learning and memory by competitively strengthening and weakening of synapses in the neural network.[100] In canonical STDP, the strength of neuron connections will increase if pre-synaptic spike arrives before post-synaptic spike within a short interval time. Conversely, the strength of neuron connections will decrease if pre-synaptic spike arrives after post-synaptic spike within a short interval time. Thus, mimicking STDP is also highly important for neuromorphic system. By modifying the spike conditions, including spike duration and amplitude, spike shapes, different kinds of STDP behaviors have been mimicked on neuromorphic devices.[24,101–103] The coexistences of multiple types of synaptic plasticity enable the design of advanced neural structures. Yin *et al.*[55] reported several types of STDP behaviors on silicon nanocrystals (Si NCs) phototransistors through combinations of light and electrical stimuli. As shown in Fig. 6(a), a symmetric Hebbian characteristic is observed when both the pre-synaptic and post-synaptic stimuli are positive V_{gs} (E^+). A symmetrical anti-Hebbian learning rule is obtained when both the pre-synaptic and post-synaptic stimuli are light stimuli (L), as shown in Fig. 6(b). Figure 6(c) shows the asymmetric Hebbian learning rule when the pre-synaptic and post-synaptic pulses are L and E^+, respectively. Finally, the device achieves asymmetric anti-Hebbian when the pre-synaptic and post-synaptic pulses are L and E^-, respectively (Fig. 6(d)).

In addition, STDP learning rules have been demonstrated with the synergistic effect of light and electrical stimuli on photoelectric synaptic devices based on 2D materials (MoS_2,[18,82] black phosphorus,[53,54]), one-dimensional nanomaterials,[59] and metal–oxide–semiconductor materials.[61] Diverse learning rules can help artificial neural networks to deal with more complex situations and improve the learning efficiency.

In physiology, classic conditioning is a typical form of associative learning in nervous system.[104] Figure 7(a) schemat-

ically shows classic Pavlovian associative learning. Initially, bell-ringing, considered as neutral stimulus (NS), can not trigger salivation. While feeding-food, considered as unconditioned stimulus (US), will activate salivation (unconditioned response, UR). During training, both US and NS are provided simultaneously, causing salivation. Thus, an association between NS and US is established. After training, NS only can cause salivation. Now, NS and UR convert to conditional stimulus (CS) and conditioned response (CR), respectively. Several groups have reported electrical stimuli triggered associative learning.[12,105–107] Moreover, Yu *et al.* have also established the relation between STDP and classic conditioning.[103] John *et al.*[82] simulated Pavlovian classic conditional reflection on a synergistic gating of electro-iono-photoactive 2D chalcogenide neuristors. The storage level of light pulses on the device is much better than that of electrical pulses. Thus, the electrical pulses were deemed as bell-ringing (Fig. 7(b)), while the light pulses were deemed as feeding-food (Fig. 7(c)). Initially, the PSC obtained by electrical pulse stimulation (NS) is less than salivation threshold of 500 nA (phase a in Fig. 7(d)). While the PSC obtained by light pulse stimulation (US) is higher than the salivation threshold (UR, phase b in Fig. 7(d)). After training for 40 cycles by applying light pulse stimulation (US) and electrical pulse stimuli (CS) together, CS only will trigger "salivation", indicating the establishment of an effective association between light pulse stimuli (feeding-food) and electrical pulse stimuli (bell-ringing). Moreover, extinction behaviors have been observed on the 2D chalcogenide neuristors. Pavlovian classical condition was also mimicked on electrolyte gated photoelectric synergic coupled oxide neuromorphic transistor with simple device configurations.[92] Light spikes are deemed as feeding food (US), while gate voltage spikes are deemed as bell ringing (NS). Moreover, Pavlovian classical condition experiments can also be simulated on synaptic devices under all-light stimulation.[54,65] These multi-input optical signal synapse devices do not need to add additional electrodes, and have a faster response speed with lower energy consumption, indicating great potentials in neuromorphic engineering.

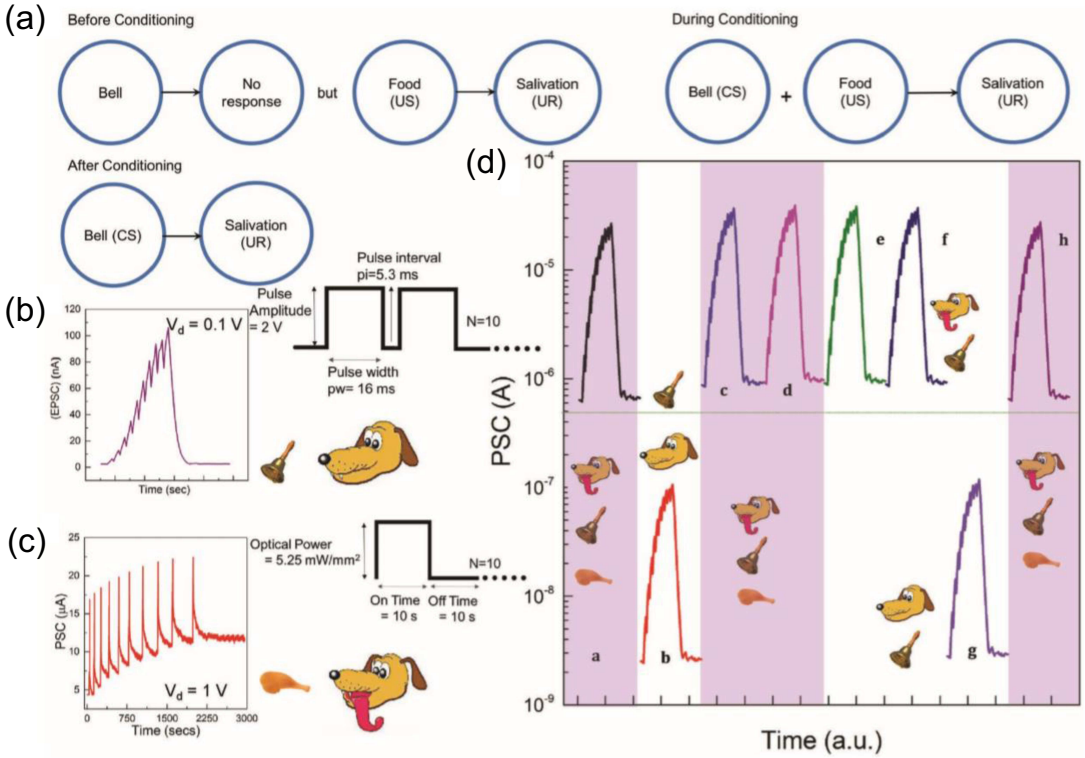


Fig. 7. Pavlovian associative learning. (a) Schematic diagram of Pavlov's dog experiment. (b) Electrical pulses as conditioned stimulus (CS) with EPSC < 500 nA (no salivation). (c) Optical pulses as unconditioned stimulus (US) with EPSC > 500 nA (salivation). (d) Imitation of Pavlovian conditioning. Reprinted with permission from Ref. [82], Copyright 2018 Wiley-VCH.

4. Artificial visual system

Up to date, various synaptic characteristics have been achieved on a single artificial synaptic device. To build an integrated system of artificial neural system may be one important branch of future neuromorphic engineering. Visual perception system is an important sensory component in bionic electronics, which can adaptively detect, process, and memorize light signals.[108] Wang *et al.*[14] fabricated a ferroelectric/electrochemical modulated organic synapse and proposed an artificial visual-perception system. There are multiple organic functional layers in the device responsible for light-sensing. Thus, the device can transducer incident light signals

into synaptic signals, both volatile and non-volatile. With the threshold property, color recognition function can be achieved. Synaptic signals triggered with light stimuli at wavelengths of 550 nm and 850 nm show different degrees of volatility. Thus, the devices demonstrate retinal functions. Lee *et al.*[109] proposed a visually sensor motor nervous system, as schematically shown in Fig. 8(a). The optical information can be sensed by photodetectors (light receptors) to generate output signals. The signals are then converted to excitatory post-synaptic current (EPSC) by a stretchable organic nanowire synaptic transistor (s-ONWST) (synapses). The EPSC is converted into a voltage signal by a transimpedance circuit to control the contraction of the polymer actuator (biological muscle). Figure 8(b) presents excellent mechanical stability of the artificial s-ONWST with flexible substrates after stretching to 100% strain. The EPSC can be modified by adjusting the trigger frequency of the action potential. Before illumination, a small voltage of $\sim$ 1 V is generated by the resting current of the artificial synapse. The artificial muscle demonstrates a slight contraction, as shown in Figs. 8(c) and 8(d). When short light pulses arrive, EPSCs are converted to voltages to operate the actuator. The output voltage and displacement δ of the actuator increase with the increasing spike number. When there are only 10 spikes, the output voltage is 1.3 V. As comparison, an output voltage of $\sim$ 3.2 V is observed with 60 spikes. Correspondingly, δ values of $\sim$ 1.5 mm and $\sim$ 2.7 mm are observed. Furthermore, the polymer actuator operated stably with s-ONWST at both 0 and 100% strains with δ at 5.3 mm and 5.4 mm, respectively. These behaviors resemble biological muscle tension responses.[110] The proposed artificial optoelectronic sensorimotion nervous system will open a new era of bioelectronic technology for the next-generation artificial limbs and soft robotics.

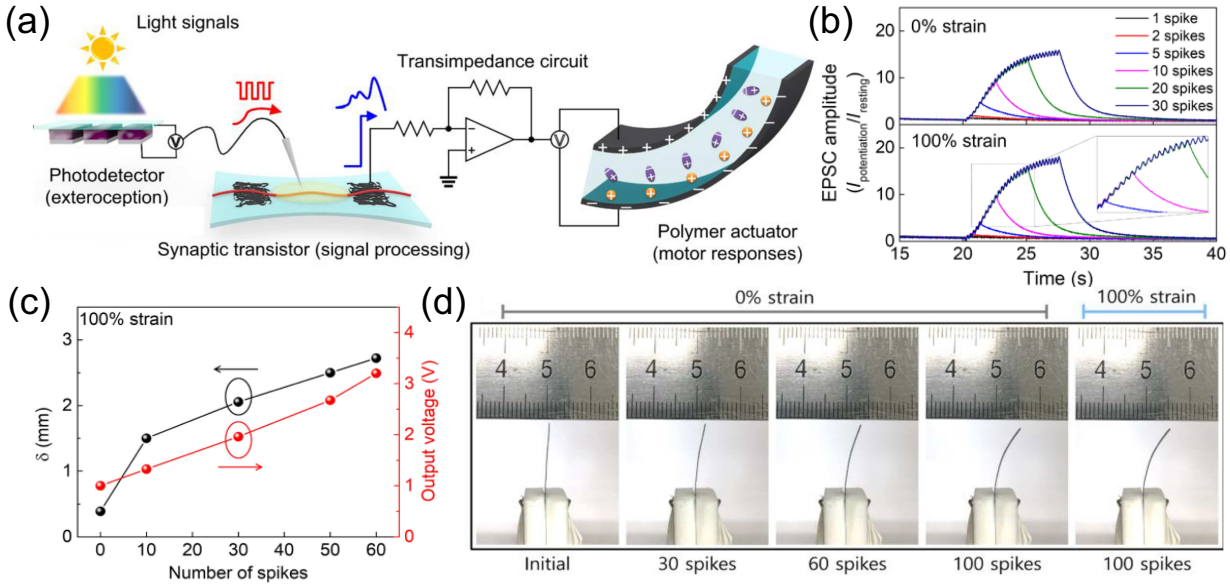


Fig. 8. Artificial sensorimotor synaptic system. (a) Schematic diagram of the visual perception motor system. (b) Spike number-dependent-plasticity (SNDP) measured on the s-ONWST. (c) Output voltage and displacement (δ) of the polymer actuator with different spike number under 100% strain. (d) Bending diagrams of polymer actuator under different spike number under 0% and 100% strain. Reprinted with permission from Ref. [109], Copyright 2018 AAAS.

5. Outlook

Neuromorphic system could be a good way to overcome Von Neumann bottleneck. Recently, several kinds of neuromorphic devices, including resistance switching devices and transistors, have been proposed to mimic basic synaptic functions, such as short-term plasticity, long-term plasticity, synaptic filtering, spike-timing-dependent plasticity, metaplasticity, heteroplasticity, etc. Moreover, advanced neuron functions have been realized, including pattern memory and pattern recognition, classical conditions, and machine learning. All these demonstrate great potentials for solid-state neuromorphic devices in neuromorphic engineering.

In addition, developing visual perception-learning system at hardware level would also provide new opportunities for advanced intelligent learning system. In such a system, advanced intelligent photodetectors play the most important role for extension of human vision. Fortunately, progresses in advanced optoelectronic devices provide these possibilities. Neuromorphic devices possessing abilities to convert light stimuli into postsynaptic signals can also simplify the visual perception-learning system. Here, we review recent progress on optoelectronic neuromorphic memristors and optoelectronic neuromorphic transistors. These optoelectronic neuromorphic devices can mimic visual perception, information processing,

and memory. Moreover, using synergistic stimuli in neuromorphic devices could significantly improve the diversity of signal inputs and the functional diversities of neural network systems and perception systems. It should be noted here that the integrated system of neuromorphic devices with artificial perception synapses and bionic electronic device with external sensory elements will have great potentials in wearable electronics, soft robots, and bionic prosthesis.

References

[1] P Yao H Q Gao W B, Eryilmaz S B, Huang X Y., Zhang W Q, Zhang Q T, Deng N, Shi L P, Wong H S P and Qian H 2017 *Nat. Commun.* **8** 15199

[2] Silver D, Hubert T, Schrittwieser J, Antonoglou I, Lai M, Guez A Lanctot M, Sifre L Kumaran D, Graepel T, Lillicrap T, Simonyan K and Hassabis D 2018 *Science* **362** 1140

[3] Liu C S, Yan X, Song X F, Ding S J, Zhang D W and Zhou P 2018 *Nat. Nanotechnol.* **13** 404

[4] Manipatruni S, Nikonov D E and Young I A 2018 *Nat. Phys.* **14** 338

[5] Drachman D A 2005 *Neurology* **64** 2004

[6] Sengupta B and Stemmler M B 2014 *Proc. IEEE* **102** 738

[7] Attwell D and Laughlin S B 2001 *J. Cereb. Blood Flow Metab.* **21** 1133

[8] Cheng Z G, Rios C, Pernice W H P, Wright C D and Bhaskaran H 2017 *Sci. Adv.* **3** 1700160

[9] Yin J, Zeng F, Wan Q, Li F, Sun Y M, Hu Y D, Liu J L, Li G Q and Pan F 2018 *Adv. Funct. Mater.* **28** 1706927

[10] Wan C J, Chen G, Fu Y M, Wang M, Matsuhisa N, Pan S W, Pan L, Yang H, Wan Q, Zhu L Q and Chen X D 2018 *Adv. Mater.* **30** 1801291

[11] Kim Y, Chortos A, Xu W T, Liu Y X, Oh J Y, Son D, Kang J, Foudeh A M, Zhu C X, Lee Y, Niu S M, Liu J, Pfattner R, Bao Z N and Lee T W 2018 *Science* **360** 998

[12] Xiong W, Zhu L Q, Ye C, Ren Z Y, Yu F, Xiao H, Xu Z, Zhou Y, Zhou H and Lu H L 2020 *Adv. Electron. Mater.* **6** 1901402

[13] Tuma T, Pantazi A, Gallo M L, Sebastian A and Eleftheriou E 2016 *Nat. Nanotechnol.* **11** 693

[14] Wang H L, Zhao Q, Ni Z J, Li Q Y, Liu H T, Yang Y C, Wang L F, Ran Y, Guo Y L, Hu W P and Liu Y Q 2018 *Adv. Mater.* **30** 1803961

[15] Kim K, Chen C L, Truong Q, Shen A M and Chen Y 2013 *Adv. Mater.* **25** 1693

[16] Zhu L Q, Wan C J, Guo L Q, Shi Y and Wan Q 2014 *Nat. Commun.* **5** 3158

[17] Huang H Y, Ge C, Zhang Q H, Liu C X, Du J Y, Li J K, Wang C, Gu L, Yang G Z and Jin K J 2019 *Adv. Funct. Mater.* **29** 1902702

[18] Jiang J, Hu W N, Xie D D, Yang J L, He J, Gao Y L and Wan Q 2019 *Nanoscale* **11** 1360

[19] Shao F, Yang Y, Zhu L Q, Feng P and Wan Q 2016 *ACS Appl. Mater. Interfaces* **8** 3050

[20] Qian C, Kong L, Yang J, Gao Y and Sun J 2017 *Appl. Phys. Lett.* **110** 083302

[21] Yu F and Zhu L Q 2019 *Phys. Status Solidi RRL* **13** 1800674

[22] Fu Y M, Wan C J, Yu F, Xiao H, Tao J, Guo Y B, Gao W T and Zhu L Q 2018 *Adv. Electron. Mate* **4** 1800371

[23] Sangwan V K, Lee H S, Bergeron H, Balla I, Beck M E, Chen K S and Hersam M C 2018 *Nature* **554** 500

[24] Xiong W, Zhu L Q, Ye C, Yu F, Ren Z Y and Ge Z Y 2019 *Adv. Electron. Mater.* **5** 1900439

[25] Ren Z Y, Zhu L Q, Guo Y B, Long T Y, Yu F, Xiao H and Lu H L 2020 *ACS Appl. Mater. Interfaces* **12** 7833

[26] Esqueda I S, Yan X D, Rutherglen C, Kane A, Cain T, Marsh P, Liu Q Z, Galatsis K, Wang H and Zhou C W 2018 *ACS Nano* **12** 7352

[27] Choi S, Tan S H, Li Z, Kim Y, Choi C, Chen P Y, Yeon H, Yu S and Kim J 2018 *Nat. Mater.* **17** 335

[28] Du C, Cai F, Zidan M A, Ma W, Lee S H and Lu W D 2017 *Nat. Commun.* **8** 2204

[29] Wan C J, Zhu L Q, Zhou J M, Shi Y and Wan Q 2014 *Nanoscale* **6** 4491

[30] Jang E K, Parka Y and Lee J S 2019 *Nanoscale* **11** 15382

[31] Gao W T, Zhu L Q, Tao J, Wan D Y, Xiao H and Yu F 2018 *ACS Appl. Mater. Interfaces* **10** 40008

[32] Lumpkin E A and Caterina M J 2007 *Nature* **445** 858

[33] Kim J, Lee M, Shim H J, Ghaffari R, Cho H R, Son D, Jung Y H, Soh M, Choi C, Jung S, Chu K, Jeon D, Lee S T, Kim J H, Choi S H, Hyeon T and Kim D H 2014 *Nat. Commun.* **5** 5747

[34] Bauer S 2013 *Nat. Mater.* **12** 871

[35] Wang G Z, Wang R B, Kong W Z and Zhang J H 2018 *Cogn. Neurodynamics* **12** 615

[36] Kwon S M, Cho S W, Kim M, Heo J S, Kim Y H and Park S K 2019 *Adv. Mater.* **31** 1906433

[37] Wang Y, Lv Z Y, Chen J R, Wang Z P, Zhou Y, L. Zhou, Chen X L and Han S T 2018 *Adv. Mater.* **30** 1802883

[38] Qian L, Sun Y L, Wu M M, Li C, Xie D, Ding L M and Shi G Q 2018 *Nanoscale* **10** 6837

[39] Hu D C, Yang R, Jiang L and Guo X 2018 *ACS Appl. Mater. Interfaces* **10** 6463

[40] Chen S, Lou Z, Chen D and Shen G Z 2018 *Adv. Mater.* **30** 1705400

[41] Liu Z, Dai S L, Wang Y, Yang B, Hao D D, Liu D P, Zhao Y W, Fang L, Ou Q Q, Jin S, Zhao J W and Huang J 2019 *Adv. Funct. Mater* **30** 1906335

[42] Qin S C, Wang F Q, Liu Y J, Wan Q, Wang X R, Xu Y B, Shi Y, Wang X M and Zhang R 2017 *2D Mater.* **4** 035022

[43] Zhai Y B, Yang X Q, Wang F, Li Z X, Ding G L, Qiu Z F, Wang Y, Zhou Y and Han S T 2018 *Adv. Mater.* **30** 1803563

[44] Zhou W, Yang R, He H K, Huang H M, Xiong J and Guo X 2018 *Appl. Phys. Lett.* **113** 061107

[45] He H K, Yang R, Zhou W, Huang H M, Xiong J, Gan L, Zhai T Y and Guo X 2018 *Small* **14** 1800079

[46] Zhou F, Zhou Z, Chen J, Choy T H, Wang J, Zhang N, Lin Z, Yu S, Kang J, Wong H S P and Chai Y 2019 *Nat. Nanotechnol.* **14** 776

[47] Kumar M, Abbas S and Kim J 2018 *ACS Appl. Mater. Interfaces* **10** 34370

[48] Yu J J, Liang L Y, Hu L X, Duan H X, Wu W H, Zhang H L, Gao J H, Zhuge F, Chang T C and Cao H T 2019 *Nano Energy* **62** 772

[49] Sun J, Oh S, Choi Y, Seo S, Oh M J, Lee M, Lee W B, Yoo P, Cho J H and Park J 2018 *Adv. Funct. Mater.* **28** 1804397

[50] Huang W, Hang P, Wang Y, Wang K, Han S, Chen Z, Peng W, Zhu Y, Xu M, Zhang Y, Fang Y, Yu X, Yang D and Pi X 2020 *Nano Energy* **73** 104790

[51] Dai S, Wu X, Liu D, Chu Y, Wang K, Yang B and Huang J 2018 *ACS Appl. Mater. Interfaces* **10** 21472

[52] Tan H, Ni Z, Peng W, Du S, Liu X, Zhao S, Li W, Ye Z, Xu M, Xu Y, Pi X and Yang D 2018 *Nano Energy* **52** 422

[53] Ahmed T, Kuriakose S, Abbas S, Spencer M J S, Rahman M A, Tahir M, Lu Y R, Sonar P, Bansal V, Bhaskaran M, Sriram S and Walia S 2019 *Adv. Funct. Mater.* **29** 1901991

[54] Ahmed T, Kuriakose S, Mayes E L H, Ramanathan R, Bansal V, Bhaskaran M, Sriram S and Walia S 2019 *Small* **15** 1900966

[55] Yin L, Han C, Zhang Q T, Ni Z Y, Zhao S Y, Wang K, Li D S, Xu M S, Wu H Q, Pi X D and Yang D R 2019 *Nano Energy* **63** 103859

[56] Luo Z D, Xia X, Yang M M, Wilson N R, Gruverman A and Alexe M 2020 *ACS Nano* **14** 746

[57] Zhai Y B, Zhou Y, Yang X Q, Wang F, Ye W B, Zhu X J, She D H, Lu W D and Han S T 2020 *Nano Energy* **67** 104262

[58] Jaafar A H, Gray R J, Verrelli E, Neill M, Kelly S M and Kemp N T 2017 *Nanoscale* **9** 17091

[59] Chen Y, Qiu W J, Wang X W, Liu W R, Wang J X, Dai G Z, Yuan Y B, Gao Y L and Sun J 2019 *Nano Energy* **62** 393

[60] Lee M, Lee W, Choi S, Jo J W, Kim J, Park S K and Kim Y H 2017 *Adv. Mater.* **29** 1700951

[61] Ma F, Zhu Y, Xu Z, Liu Y, Zheng X, Ju S, Li Q, Ni Z, Hu H, Chai Y, Wu C, Kim T W and Li F 2020 *Adv. Funct. Mater.* **30** 1908901

[62] Lv Z, Chen M, Qian F, Roy V A L, Ye W, She D, Wang Y, Xu Z X, Zhou Y and Han S T 2019 *Adv. Funct. Mater.* **29** 1902374

[63] Zhao J, Zhou Z, Wang H, Wang J, Hao W, Ren D, Guo R, Chen J, Liu B and Yan X 2019 *Appl. Phys. Lett.* **115** 153504

[64] Murdoch B J, Raeber T J, Zhao Z C, Barlow A J, McKenzie D R, McCulloch D G and Partridge J G 2019 *Carbon* **152** 59

[65] He W X, Fang Y, Yang H H, Wu X M, He L H, Chen H P and Guo T L 2019 *J. Mater. Chem. C* **7** 12523

[66] Chua L O 1971 *IEEE Transactions on circuit theory* **18** 507

[67] Strukov D B, Snider G S, Stewart D R and Williams R S 2008 *Nature* **453** 80

[68] Kuzum D, Jeyasingh R G D, Lee B and Wong H S P 2012 *Nano Lett.* **12** 2179
[69] Gao S, Liu G, Yang H L, Hu C, Chen Q L, Gong G D, Xue W H, Yi X H, Shang J and Li R W 2019 *ACS Nano* **13** 2634
[70] Yang Y C, Zhang X X, Qin L, Zeng Q B, Qiu X H and Huang R 2017 *Nat. Commun.* **8** 15173
[71] Son D, Chae S I, Kim M, Choi M K, Yang J, Park K, Kale V S, Koo J H, Choi C, Lee M, Kim J H, Hyeon T and Kim D H 2016 *Adv. Mater.* **28** 9326
[72] Zucker R S and Regehr W G 2002 *Annu. Rev. Physiol.* **64** 355
[73] Lee C H, Lee G H, Zande A M, Chen W C, Li Y L, Han M Y, Cui X, Arefe G, Nuckolls C, Heinz T F, Guo J, Hone J and Kim P 2014 *Nat. Nanotechnol.* **9** 676
[74] Wang Q H, Kalantar-Zadeh K, Kis A, Coleman J N and Strano M S 2012 *Nat. Nanotechnol.* **7** 699
[75] Liu B, Li C X, Yang P P, Hou Z Y and Lin J 2017 *Adv. Mater.* **29** 1605434
[76] Mennel L, Symonowicz J, Wachter S, Polyushkin D K, Molina-Mendoza A J and Mueller T 2020 *Nature* **579** 62
[77] Diorio C, Hasler P, Minch A and Mead C A 1996 *IEEE Trans. Electron Devices* **43** 1972
[78] Zhu L Q, Xiao H, Liu Y H, Wan C J, Shi Y and Wan Q 2015 *Appl. Phy. Lett.* **107** 143502
[79] Wan C J, Zhu L Q, Liu Y H, Feng P, Liu Z P, Cao H L, Xiao P, Shi Y and Wan Q 2016 *Adv. Mater.* **28** 3557
[80] Kim S G, Kim S H, Park J, Kim G S, Park J H, Saraswat K C, Kim J and Yu H Y 2019 *ACS Nano* **13** 10294
[81] Wang K, Dai S L, Zhao Y W, Wang Y, Liu C and Huang J 2019 *Small* **15** 1900010
[82] John R A, Liu F C, Chien N A, Kulkarni M R, Zhu C, Fu Q D, Basu A, Liu Z and Mathews N 2018 *Adv. Mater.* **30** 1800220
[83] Wang S Y, Chen C S, Yu Z H, He Y L, Chen X Y, Wan Q, Shi Y, Zhang D W, Zhou H, Wang X R and Zhou P 2019 *Adv. Mater.* **31** 1806227
[84] Eccles J C 1964 *The Physiology of Synapses* (New York: Academic Press) p. 189215
[85] Fu Y M, Zhu L Q, Wen J, Xiao H and Liu R 2017 *J. Appl. Phys.* **121** 205301
[86] Im M, Werginz P and Fried S I 2018 *J. Neural. Eng.* **15** 036010
[87] Ohno T, Hasegawa T, Tsuruoka T, Terabe K, Gimzewski J K and Aono M 2011 *Nat. Mater.* **10** 591
[88] Lu A, Sun J, Jiang J and Wan Q 2010 *Appl. Phys. Lett.* **96** 043114
[89] Hong K, Kim S H, Lee K H and Frisbie C D 2013 *Adv. Mater.* **25** 3413
[90] Zhu L Q, Chao J Y and Xiao H 2014 *Appl. Phys. Lett.* **105** 243508
[91] Zhu Y X, Liu G X, Xin Z J, Fu C Y, Wan Q and Shan F K 2020 *ACS Appl. Mater. Interfaces* **12** 1061
[92] Guo Y B, Zhu L Q, Long T Y, Wan D Y and Ren Z Y 2020 *J. Mater. Chem. C* **8** 2780
[93] Cash S and Yuste R 1999 *Neuron* **22** 383
[94] Atkinson R C and Shiffrin R M 1968 *Psychol. Learn. Motiv.* **2** 89
[95] Yu F, Zhu L Q, Gao W T, Fu Y M, Xiao H, Tao J and Zhou J M 2018 *ACS Appl. Mater. Interfaces* **10** 16881
[96] Tian H, Cao X, Xie Y J, Yan X D, Kostelec A, DiMarzio D, Chang C, Zhao L D, Wu W, Tice J, Cha J J, Guo J and Wang H 2017 *ACS Nano* **11** 7156
[97] Qian C, Oh S, Choi Y, Kim J H, Sun J, Huang H, Yang J L, Gao Y L, Park J H and Cho J H 2019 *Nano Energy* **66** 104095
[98] Feldman D E 2012 *Neuron* **75** 556
[99] Tsukada M, Yamazaki Y and Kojima H 2007 *Cogn. Neurodynamics* **1** 157
[100] Song S, Miller K D and Abbott L F 2000 *Nat. Neurosci.* **3** 919
[101] Li Y, Zhong Y P, Xu L, Zhang J J, Xu X H, Sun H J and Miao X S 2013 *Sci. Rep.* **3** 1619
[102] Li Y, Zhong Y P, Zhang J J, Xu L, Wang Q, Sun H J, Tong H, Cheng X M and Miao X S 2014 *Sci. Rep.* **4** 4906
[103] Yu F, Zhu L Q, Xiao H, Gao W T and Guo Y B 2018 *Adv. Funct. Mater.* **28** 1804025
[104] Fanselow M S and Poulos A M 2005 *Annu. Rev. Psychol.* **56** 207
[105] Tan Z H, Yin X B, Yang R, Mi S B, Jia C L and Guo X 2017 *Sci. Rep.* **7** 713
[106] John R A, Tiwari N, Chen Y Y, Ankit, Tiwari N, Kulkarni M, Nirmal A, Nguyen A C, Basu A and Mathews N 2018 *ACS Nano* **12** 11263
[107] Li Y, Xu L, Zhong Y P, Zhou Y X, Zhong S J, Hu Y Z, Chua L O and Miao X S 2015 *Adv. Electron. Mater.* **1** 1500125
[108] Lee G J, Choi C, Kim D H and Song Y M 2018 *Adv. Funct. Mater.* **28** 1705202
[109] Lee Y, Oh J Y, Xu W, Kim O, Kim T R, Kang J, Kim Y, Son D, Tok J B H, Park M J, Bao Z N and Lee T W 2018 *Sci. Adv.* **4** eaat7387
[110] Head S I and Arber M B 2013 *Adv. Physiol. Educ.* **37** 405